International Journal of Control, Automation and Systems 19(2) (2021) 1054-1064
http://dx.doi.org/10.1007/s12555-019-0859-x
ISSN:1598-6446 eISSN:2005-4092
http://www.springer.com/12555

A Series-elastic Robot for Back-pain Rehabilitation

ElHussein Shata, Kim-Doang Nguyen*, Praneel Acharya, and Jeffrey Doom

Abstract: This paper addresses the robot-assisted rehabilitation of back pain, an epidemic health problem affecting a large portion of the population. The design is composed of two springs in series connected to an end-effector via a pair of antagonistic cables. The spring and cable arrangement forms an elastic coupling from the actuator to the output shaft. An input-output torque model of the series-elastic mechanism is established and studied numerically. The study also illustrates the variation of the mechanism's effective stiffness by changing the springs' position. In addition, we built a prototype of the robotic mechanism and design experiments with a robotic manipulator to experimentally investigate its dynamic characteristics. The experimental results confirm the predicted elasticity between the input motion and the output torque at the end-effector. We also observe an agreement between the data generated by the torque model and data collected from the experiments. An experiment with a full-scale robot and a human subject is carried out to investigate the human-robot interaction and the mechanism behavior.

Keywords: Back-pain rehabilitation, experimental validation, torque models, variable stiffness actuators.

1. INTRODUCTION

1.1. Background on back-pain

Back pain is one of the most epidemical health problems [1]. Up to 80% of all people suffer from this spinal musculoskeletal disorder (SMD) at some point in life [2]. Back pain affects different parts of the body including shoulders, neck and especially upper and lower back. Among these, low back pain, also known as lumbago [3], is one of the most common syndromes that occur at various ages. It is a major cause for disability, also the second leading cause of activity limitation and sick leave throughout the world [4]. One common cause leading to lower back pain is due to activities involving carrying heavy loads. In such cases, the connective fibers of ligaments and tendons can begin to adhere to each other and lose resilience and may also tear down when a sudden overload occurs. Since muscles are in constant communication with the central nervous system [5], ongoing tension prevents normal muscle functions and lead to muscle spasms and further stability problems, which in turn can lead to chronic lower back pain and disability [6].

Recovery from back pain is slow and uncertain [7]. A recent study in [1] reported that about $60-70\%$ of patients recover within 6 weeks, and $80-90\%$ recuperate within 12 weeks with some help of rehabilitative therapy. However, after 12 weeks, back pain becomes chronic and leads to periods of intense pain, significant physical limitations, and activity impairment. Those who do not recover by 12 weeks account for up to 90% of total expenses related to this health-care problem. For example, the expenses exceed $90 billion/year in the U.S. [8], $8.1 billion/year in Canada [9], and $9.17 billion/year in Australia [10].

The correlation between SMDs and motor control has been widely reported [11]. Rehabilitative therapy for the spine is essential for back-pain patients to regain their spinal mobility. Structured and repetitive exercises that result in bodily movement and energy expenditure by activation of skeletal muscles has proved to be effective for the recovery of functional spinal motor skills [12]. For instance, sit-up exercises, knee extension, cat-stretch, and aerobics would assist in back-pain recovery [13]. However, patients who are subjected to back pain disorders have challenges and difficulties in performing these tasks.

Current rehabilitative techniques for back pain require intensive, subjective assessment of motor function, and therapeutic procedures supervised by a team of physiotherapists [14]. In addition, the current practice lacks quantification in instructing patients as well as in the monitoring of rehabilitative progress. This hinders the design of the therapeutic procedures that fit patient characteristics and the prediction of therapy success. Finally, rehabilitation programs for back pain patients are excessively costly and are restricted to hospital environments.

Manuscript received October 9, 2019; revised March 7, 2020 and April 14, 2020; accepted June 8, 2020. Recommended by Associate Editor Yangmin Li under the direction of Editor Doo Yong Lee. This work is supported by the FY20 Competitive Research Grant Program of South Dakota Board of Regents.

ElHussein Shata, Kim-Doang Nguyen, Praneel Acharya, and Jeffrey Doom are with the Department of Mechanical Engineering, South Dakota State University, USA (e-mails: {Elhussein.Shata, Doang.Nguyen, Praneel.Acharya, Jeffrey.Doom}@sdstate.edu).
* Corresponding author.

Robot-assisted rehabilitation therapy is an emerging approach for musculoskeletal disorder treatment after neurologic injuries such as stroke and spinal cord injury. Robotic devices can help patients achieve the intensive, repetitive practice needed to stimulate neural recovery, reduce the need for supervision, and improve cost-benefit profiles [15]. Most recent research focuses on robotic assistive devices for the recovery of functional upper and lower limbs [16]. The few existing robotic systems for back-pain rehabilitation (see [17], for example) tend to override the user's motion. They are designed with rigid links and joints and do not account for the neuromotor delays in the musculoskeletal systems [18]. In this paper, we bridge these gaps in rehabilitation robotics by:

- Designing a bio-assistive device that assists in the rehabilitation of back pain patients.
- Ensuring the elasticity of the system to accommodate unintentional movements from the patient.
- Varying the stiffness of the mechanism when desired to achieve the required resistance.
- Validating the proposed design through experiments with a full-scale robot and a human subject.

The compliant actuator that drives the device works by restoring a desired position and creating an adjusted resistance accordingly. This movement, with the assistance of the mechanism, will help increase the strength in the muscles that function to stabilize or mobilize the spinal column. The device will offer the amount of motor practice needed to relearn spinal motor skills with less therapist assistance. In addition, the compliant design of the robotic rehabilitator will guarantee safe interactions between a patient and the robot during a rehabilitative session due to the elastic component that is integrated in the design. This device will be one of the very few robotic systems that assist in the recovery of patients with severe back.

1.2. Background on elastic actuators

Robotic rehabilitators are essentially mechanical structure-based devices built for physical rehabilitation. Since these robots are designed to share a common space and proximity to participants, the users' safety is a major concern. In addition, the rehabilitative mechanism used must accommodate for any uncontrollable or involuntary movements produced by patients due to musculoskeletal disorders. To address these concerns, adding compliant elements to traditional rigid link-joint mechanisms has proved to be an efficient way to inherently reduce the risk of accidents in human-robot interactions and minimize the effect of high-frequency involuntary movements [19].

In general, series-elastic actuators (SEA) can be categorized into three types depending on the springs' configurations (see Fig. 1):

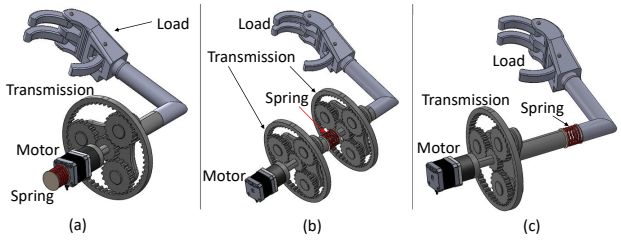

Fig. 1. Three configurations of a series-elastic actuator: (a) RFSEA, (b) TFSEA, and (c) FSEA.

- Reaction Force Sensing Series Elastic Actuator (RFSEA) - where the spring is positioned before or after the motor, for example, the mechanism in [20],
- Transmitted Force Sensing Series Elastic Actuator (TFSEA) - the spring is positioned between the gearboxes, for example, the mechanism in [21],
- Force-sensing Series Elastic Actuator (FSEA) - the spring is positioned after the force transmission and before the applied load, for example, the one in [23].

There are many variable stiffness actuators that are tangential to the above three categories of elastic actuators. For instance, via a special arrangement of springs, a belt, and two motors, work in [19] shows that it is possible to vary the effective stiffness and impedance properties of the elastic actuators. Another example is the hybrid variable stiffness actuator in [24], which is based on the adjustable moment-arm principle. The mechanism can switch between a rigid mode, in which it works like a traditional rigid joint, and an elastic mode with a wide range of stiffness depending on the length of the moment arm. Similarly in [25] that is a Rotary Flexible Joint that can be used in many applications. The Mechanically Adjustable Compliance and Controllable Equilibrium Position Actuator (MACCEPA) [36] was originally designed for a biped robot. It is then adopted for many other legged robots. This work develops a clever procedure for establishing the torque model, which is leveraged in our paper to establish our own force model.

Through the brief review above, there have been many phenomenal design innovations that facilitate elastic couplings in actuation systems. However, these design principles have been mostly applied to enable the locomotion of legged robots and rehabilitation robots for limbs. They have not been used to design a rehabilitation robot for the recovery of back pain. Motivated by this, this paper develops a series-elastic actuating mechanism for back-pain physical rehabilitation.

The rest of this paper is organized as follows: Section 2 describes the bio-inspired design of the mechanism including the requirements, working principle, and a CAD model for the proposed mechanism. In Section 3, we construct a torque model of the mechanism and show that the mechanism is capable of varying its effective stiffness by

adjusting the positions of the springs. We discuss the effects of each parameter in the elastic actuation system. In Section 4, a small-scale prototype of the mechanism is fabricated and presented. In this section, we also discuss the experimental set-up and analyze the experimental results that validate the theoretical torque model. Section 5 discusses the experimental results with a full-size robot assisting a human subject in a set-up exercise. Finally, Section 6 gives several concluding remarks.

2. DESIGN

2.1. Design requirements specification

In designing a rehabilitation robot, clinical acceptance relies on the added value in offering features or functions difficult to achieve with conventional therapy [26]. Features such as exact repetitive movements, adjustable resistance, and movement sensing capabilities would theoretically increase clinical acceptance [27]. The systems on the market are large, expensive, not portable and intended only for clinic use with therapy staff present. Additionally, the cost includes system maintenance and training [28].

During a rehabilitation session, a patient is an integral part of the robotic mechanism where the robot senses the command motion of the patient and provides assistance in terms of effort [29]. This helps the patient complete an exercise to promote their active movement and improve the motor function recovery. The main requirement in the development of such a robotic rehabilitator is that safe interactions between a human user and the bio-assistive device must be absolutely ensured [30]. This challenge is the fundamental motivation for the robot design in this paper.

In gym equipment, elastic coupling belts are commonly used, likewise in rehabilitation of human arms [31], which partially absorb unintentional or instinctive actions produced by users and reduce injury risk to users. Inspired by this, our design is based on a cable-driven elastic coupling between an actuator and an end-effector that interact with a user. An elastic coupling actuator with adaptable compliance can be modeled as spring driven by a cable of which both the force in the cable and the position of the springs can be controlled separately. Furthermore, one of the requirements for the proposed design is that the torque applied on the springs should be zero when there is no spring displacement, and the torque should be symmetrical around the equilibrium position. In the design, the springs can gradually manipulate their position to change the formed stiffness as needed to meet the necessity of the patient, therefore the control of the equilibrium position and the compliance is completely independent. The mechanism should be simple, easy to use and control. Simplicity results mostly in sturdiness and low-cost designs.

2.2. Design principles

Exercise therapy is a management strategy that is widely used in low-back pain. It encompasses a diverse group of involvements ranging from general physical fitness or aerobic exercises to muscle strengthening. Repetitive exercises have proven to be an effective method for back pain treatment [34]. Partial crunches, for instance, can help strengthen the muscles around the spine, therefore, reinforce the back [35]. However, patients with chronic back pain would have challenges performing these exercises without assistance. Also, sit-up exercises require assistance for back pain patients to accomplish. Various types of flexibility and stretching exercises that can treat lumbago patients, but they require a helping hand and lack the assistance element. Current assistive systems used in physiotherapy clinics such as Isostation B200 [37] or other exercise devices such as [38] lack the ability to vary stiffness. Therefore, there is a need for a therapeutic system that can be designed to integrate robotics and mechatronics to develop an intelligent responsive robotic system. Such robots can provide a useful aid for the therapist in performing repetitive tasks of the treatment program, and in assisting the patient and the therapist to achieve progressive results.

Most of the rehabilitation devices do not accommodate therapeutic resistance [32]. The few existing robotic systems for back-pain rehabilitation are designed with rigid joints and tend to override the user's motion [33]. To address this gap, we design the robotic mechanism following the principle of series-elastic actuation, in which the compliant element's stiffness is variable. Traditional actuation systems are designed such that the interface between the motor shaft and the payload is as stiff as possible, and is usually a rigid coupling, like most industrial manipulators. In contrast to rigid coupling actuators, a variable-stiffness actuator is installed with an elastic interface between the motor output and the payload.

Variable-stiffness actuators offer many advantages especially to a rehabilitation robot that physically interacts with human users. Firstly, since the patient and the device perform a therapeutic exercise for musculoskeletal recovery in collaboration, low-stiffness joints, and low reflected inertia reduce the risk of the robot hurting the participant. In addition, variable impedance actuators offer better accessibility to haptic feedback, and therefore, may achieve more accurate and stable force control. Moreover, the elastic couplings partially absorb uncontrollable or involuntary movements often produced by patients with spinal musculoskeletal disorders. The residual vibrations will be actively isolated by the control algorithm of the rehabilitator. This is important because we want the robotic system to provide force and movement assistance that is as stable as possible during operation.

2.3. Conceptual design

Fig. 2 shows the conceptual design of the back-pain rehabilitation robot prototype. We use a crank-slider mecha-

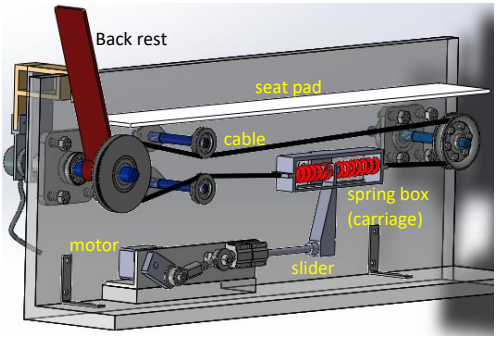

Fig. 2. CAD model of the proposed design.

nism to convert the motor's rotation to a slider's linear motion, which drives a carriage via a combination of springs and dampers (spring box). Both slider and carriage are constrained to only move horizontally. The motion of the carriage then pulls an antagonistic pair of cables to rotate the joint as shown in the kinematic diagram.

This design is inspired by the antagonistic pairs of muscles found in many animals. The mechanism set-up forms a compliant coupling between the motor shaft and the joint, which guarantees safe human-robot interactions when the patient and the device perform a therapeutic exercise for musculoskeletal recovery in collaboration. The design offers accessibility to haptic feedback by measuring the spring displacements, and therefore, may achieve more accurate and stable force control. Furthermore, the mechanism is so versatile that it is compatible with different therapeutic exercises. In particular, Fig. 3 shows two configurations with slightly different end-effector designs: one for sit-up exercises and the other for knee extension exercises, which are some of the most common exercises for back-pain rehabilitation. As seen in both configurations, two springs are installed in a box and are connected in series to a shaft to enable elastic couplings in both directions. The vertical position of the other two ends of the springs can be adjusted to change the effective stiffness of the elastic coupling. This adjustment to the spring positions is equivalent to changing B and E as seen in Fig. 4. To ensure force transition, a cable is deployed and is connected to each side of the spring box and can rotate around two pulleys, one of which is idle and the other drive the end-effector that interact with a user. The length of the cable is always constant. Once the drive shaft H moves horizontally with a velocity $\dot{x}$, it will result in an instantaneous displacement Δx for Spring 1 and $-\Delta x$ for Spring 2. As the spring box is designed to respond to the drive shaft motion, it will only move horizontally, i.e. to the left or to the right depending on the elastic force direction. As a result, tension will be generated in one side of the cable, generating an angular displacement of Pulley 1, and hence of the end-effector that provides the assisting force for the user. For instance, when the driving shaft moves to the right, Spring 1 is extended and Spring 2 is compressed, the

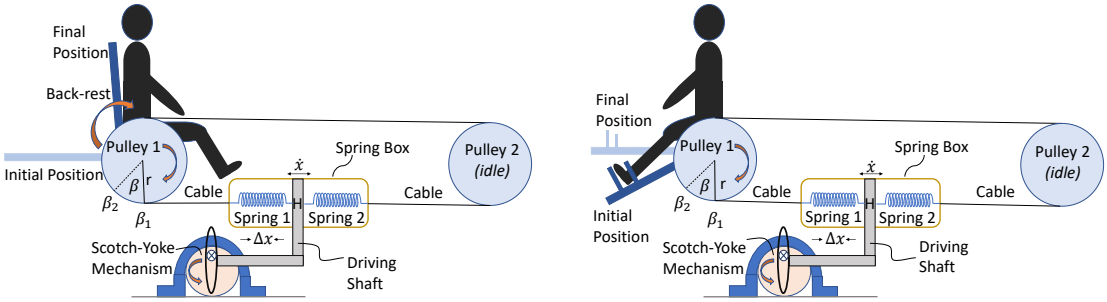

(a) Sit-up configuration.

(b) Knee-extension configuration.

Fig. 3. The conceptual design of the proposed elastic coupling in two configurations.

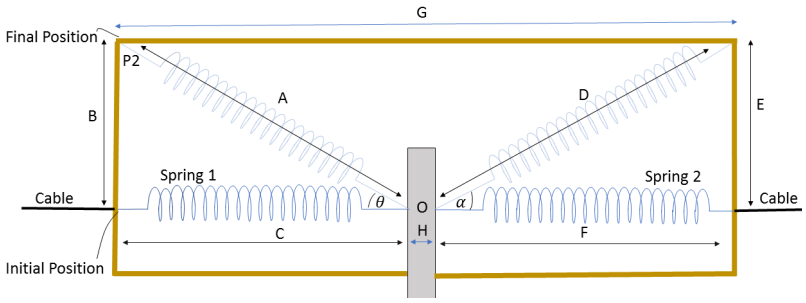

Fig. 4. The spring box that facilitate variable stiffness by changing the position of the springs.

bottom cable is under tension, and the end-effector is displaced in the counterclockwise direction, and vice versa.

This design system accommodates the variation of the effective stiffness of the elastic coupling from the torque produced by the motor to the torque acting at the end-effector that interacts with a user. This stiffness variability enables a change in the level of physical assistance or resistance to match individual users and their stage in back-pain recovery. There is a torque model that governs the relationship between the actuator's motion and the output torque acting on the user. In the next section, we will have a deeper look into this torque model and the principle for varying the effective stiffness of the proposed design.

3. TORQUE MODEL

As discussed earlier, the designed mechanism facilitates the capability of changing the geometry of the spring arrangement, resulting in a variable stiffness actuation mechanism. A zoomed-in illustrative diagram for the spring box is shown in Fig. 4 that conceptually depicts this idea. The fundamental hypothesis is that when the positions of the ends of the two spring are changed, the dependence of the output torque at the end-effector and the input motor's motion will change accordingly. Therefore, the resultant vertical positions of the springs will create two new variables to control, theta (θ) and alpha (α). This will eventually result in an adjustable compliance output. To validate this hypothesis, we will first establish a torque model with the position of the springs being variables.

3.1. Nomenclature

All variables and parameters are defined as follows:

β = Angular displacement of Pulley 1
A and D = Hypotenuse displacement of Springs 1 and 2
B and E = Opposite displacement of Springs 1 and 2
C and F = Adjacent displacement of Spring 1 and 2
θ and α= Angular displacement of Spring 1 and 2
G = Total length of the Spring Box
H = Driving shaft's thickness
F_{in} = Initial spring force of Spring n
T_f = Total frictional torque
L_{i0} = Natural length of Spring i
k = Spring stiffness
Δx = Linear displacement of the spring
r = Pulley radius
T_i = Torque generated due to Spring i
T = Total torque generated

3.2. Derivation

We will first analyze the force model of Spring 1 and that of Spring 2 will follow accordingly due to the symmetry of the spring box which is shown in Fig. 4. The torque produced at the shaft of Pulley 1 (the end-effector) is the total torque of the system due to the net displacement of both springs. We consider the input of the torque model to be the spring displacement Δx, and the output to be the torque T generated on the rotating joint (the driving shaft). At initial position of Spring 1, $\theta = 0^o$ and $\Delta x = C - L_{10}$. Applying Hooke's law, the elastic force of Spring 1 at initial configuration can be obtained as follows:

$$F_{i1} = k(C - L_{10}). \tag{1}$$

Indeed, this is the equation governing a linear force relationship of a traditional series-elastic actuation mechanism, in which the stiffness is exactly k.

At an arbitrary position θ, we have $\Delta x = A - L_{10} = \sqrt{C^2 + B^2} - L_{10}$. It follows that the spring force can be obtained as

$$F_1 = k(\sqrt{C^2 + B^2} - L_{10}). \tag{2}$$

This elastic force due to Spring 1 at an arbitrary configuration can be expressed into two components: one acting horizontally and the other acting vertically to the spring box. The horizontal component is simply $F_{1x} = F_1 \cos(\theta)$, which is transmitted along the cable and acts on the end-effector causing the following torque:

$$T_1 = rkC(1 - \frac{L_{10}}{\sqrt{C^2 + B^2}}). \tag{3}$$

As mentioned earlier, the effect of Spring 2 can be obtained following a similar approach for Spring 1. Thus, accounting for the effect of both springs, and assuming T_f is the total frictional torque along the components' movements, we obtain the total torque:

$$T = rk[C(1 - \frac{L_{10}}{\sqrt{C^2 + B^2}}) - F(1 - \frac{L_{20}}{\sqrt{F^2 + E^2}})] - T_f, \tag{4}$$

where $F = G - H - C$. Equation (4) is the torque model that governs the torque produced by the mechanism at the end-effector in response to a displacement C and F (but these are dependent) of the springs produced by the motor's input motion. The effective stuffness of the elastic coupling can be varied by adjusting B and E as shown in the equation. While this model is nonlinear in C and F, it recovers the linear form in (1) when $B = E = 0$.

3.3. Influence of design variables

In this section, the influence of design variables will be investigated and simulated. To better study the mechanism, the variables k, G, L_{10} and L_{20} are chosen during the design and are fixed during normal operation. We set $B = E$ for simplicity and change their values after each experiment. We aim to illustrate that by changing B and E, we are able to obtain different effective stiffness, therefore variable-stiffness property of the proposed design.

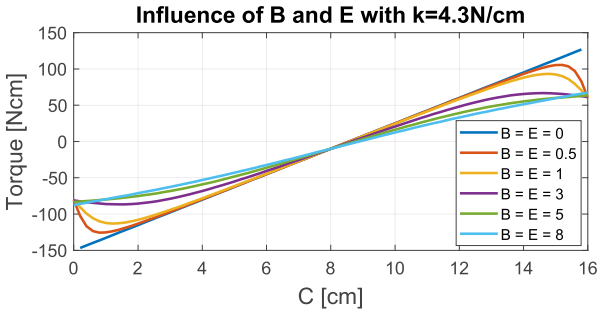

Fig. 5. Dependence of the output torque on the spring displacement for different positions of the springs.

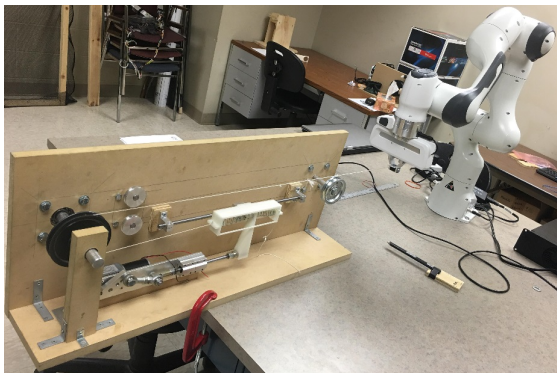

Fig. 6. Experimental setup with the fabricated prototype of the series-elastic mechanism for back-pain rehabilitation and a robotic manipulator.

The natural length of both springs (L_{10} and L_{20}) is 8 cm. In each experiment, we vary the spring displacement C and employ the torque model in (4) to calculate the torque. The results from these numerical experiments are shown in Fig. 5. We can see from these figures that the effect of the spring position is evident. When $B = E = 0$, the model produce a straight line corresponding to a linear torque relationship in traditional series-elastic actuators as discussed earlier. When B and E are increased, the model displays clear nonlinearity proportionally. This variation confirms our hypothesis stated earlier.

The dependence of the torque on the spring displacement is depicted in Fig. 5. For every curve, since when $C = 8$ cm, the springs are at their natural length, the mechanism produces no torque. When $C \in [2,8)$, Spring 1 is compressed while Spring 2 is extended. The torque is acting in the clockwise direction, and hence is negative. Pulley 1 along with the end-effector are moving in the clockwise direction. The opposite trend is observed when $C \in (8,16]$. It is worth noting that the torque model derived in (4) not only depends on the spring displacements C and F as shown explicitly, it is also a function of the angular displacement of the springs, α and θ, implicitly.

In order to validate the properties discussed in Section 3, we built a prototype of this series-elastic actuation mechanism in a back-pain rehabilitation robot and analyze the experimental results in the following section.

4. EXPERIMENT

Fig. 6 shows the prototype of the series-elastic actuation mechanism for a back-pain rehabilitation robot. Initially, we design this prototype to test the validity of the mechanism. The frame used to serve as our main plane is made from wood and has dimensions of 81 cm wide and 31.75 cm tall. The motor's maximum speed is 35 RPM. The carriage (spring box) is 17.78 cm long and 3 cm wide. The springs used are 1.8 cm diameter and 8 cm long. The vertical link that is driving the springs is 12 cm tall and 2 cm wide. Moreover, the idle pulley on the right is 7.32 cm in diameter, and the driving pulley on the left is 10 cm in diameter. The total length of the cable is 132 cm and the driving shaft is 2 cm in diameter.

A linear actuator is designed with a crank driven by a programmable DC motor. The crank's rotary motion is transmitted to a slider via a coupler link and two revolute joints. The slider's linear motion is supported by linear bearings and drive the motion of a vertical shaft. The other end of the shaft is mounted to two springs each of which is on one side as shown. The other ends of the two spring are connected to a 3D printed box's walls. The entire spring box is supported by another set of linear bearings, that constrains the box to move along the horizontal direction. The outsides of the spring box's walls are attached to two polymer cables, whose ends are mounted to the pulley. The cable drives the end-effector that interact with a user. The end-effector is the back-rest pad for sit-up exercises or it can be the leg-rest pad for knee-extension exercises. The cables' tension is maintained by three idle pulleys, each of which is supported by a shaft inserted into a bearing flange mounted to the wooden support frame. Each cable pulls the output pulley in an opposite direction, for example, if the top cable is pulling, the end-effector rotate in the clockwise direction, while if the bottom cable is pulling, the end-effector rotates in the counterclockwise direction. The range of motion of the slider in the linear actuator is $2r_{crank}$. We want the range of motion of the end-effector to be 90°, which is equivalent to the cable range (i.e. circumference) of $(1/4)2\pi r_{pulley}$. Therefore, the size of the output pulley is designed as

$$r_{pulley} = (4r_{crank}/\pi). \tag{5}$$

The springs used in this design are compression springs with a coil thickness of 1.05 mm, the total diameter of 18.26 mm, and the total length of 80 mm. For this initial prototype, the compliance is fixed without changing the angular position of the springs. To capture the motion of the end-effector, an encoder is attached to the rotational axis of the shaft that is driving the output pulley and the

end-effector. The encoder is a Signswise's incremental rotary encoder with 600 pulses per revolution. A Microchip ATMEGA 2560 microcontroller is used to program the motor and record the analog angle information produced from the rotary encoder. Through a serial communication interface, the data are exchanged between the controller and a computer for further analysis.

In the experiments, we validate the torque model established in (4). This experiment focuses on examining the linear elastic behavior of the mechanism and the output torque due to various spring displacement. A seven axial robotic manipulator is used to provide and measure the precise displacements of the spring as shown in Fig. 6. Moreover, the robot arm is embedded with force-torque sensors in all of its joints so it facilitates the measurements of the force applied onto its end-effector. The manipulator's end-effector is attached to the cable to pull and release the output pulley and therefore move the spring box accordingly. The entire series-elastic actuation mechanism is clamped on a stationary table that is the base of the manipulator.

Each experiment was divided into two segments. The first segment was to tension Spring 1 while compressing Spring 2. The manipulator pulled the output pulley in the clockwise direction, and the spring box was moving horizontally to the left. Spring 1 was tensioned up to 10 cm, while Spring 2 was compressed to 6 cm. The second segment was to compress Spring 1 and tension Spring 2. The manipulator was pulling the output pulley in the counterclockwise direction, and the spring box was moving horizontally to the right. Spring 1 was compressed down to 6 cm, while Spring 2 was tensioned to 10 cm.

The experiment was done ten times. The displacement for each spring was measured every 2 mm and the output force required to move the mechanism this displacement was obtained from the robot's sensors and software. The data was then filtered to include all the data points collected that are between 6 cm to 10 cm. The spring stiffness was also calibrated based on the same experiment.

Fig. 7 shows all the experimental data plotted for the ten runs, along with the model data points computed using the torque model derived in (4). In this figure, the back dashed line indicates the data computed by the torque model in (4), while other solid lines are data collected from the ten experiments. The data are summarized in Fig. 7 that shows the mean and standard deviations. From these data figures, we can see that the torque produced by the theoretical torque model is close to those measured from the experiments both in terms of the trend and the mean values. The small gap between the two sets of data stems from the fact that the theoretical model does not take into account the effect of friction, while the friction forces influence the experimental data. In addition, the imperfect calibration of the spring stiffness is another source for the mismatch observed in these data figures.

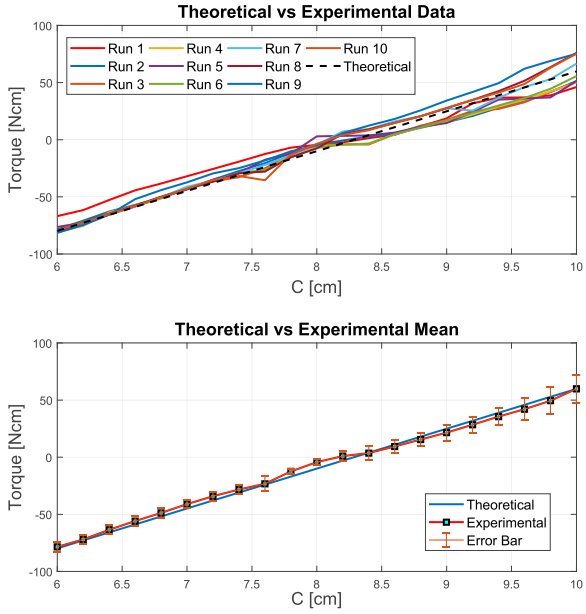

Fig. 7. Experimental data: measured torque versus spring displacement.

5. EXPERIMENTS WITH A HUMAN SUBJECT

To conduct an experiment of the proposed robot design interacting with a human subject, a full-size robot was built as shown in Fig. 8. These experiments aim to demonstrate the interaction profile in terms of force acting from the robot end-effector to the participant's back. A matrix of 14 force sensors, including 7 rows and 2 columns, was mounted on the back-pad. A Signswise's incremental ro-

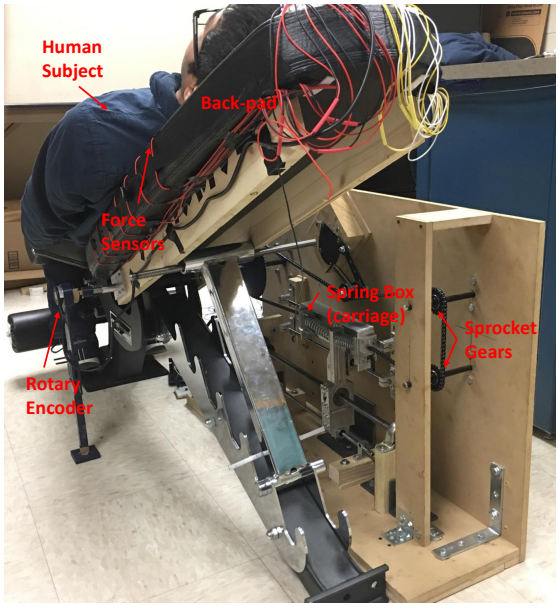

Fig. 8. Experiment set-up with a full-size rehabilitation robot and a human subject.

tary encoder is attached to the output shaft that drives the back-pad shown in Fig. 8 to measure the end-effector's angular motion. The force sensors and the encoder's data are both collected with a Microchip ATMEGA 2560 microcontroller. A Nema 34-step motor was used to actuate the mechanism. The stepper motor can produce a torque of up to 13 Nm (1841 oz-in) and is commanded by a digital stepping driver DM860I. The stepper motor and the driver are both controlled by a Microchip ATMEGA 328P microcontroller. The full-size rehabilitation robot has dimensions of $84 \times 56 \times 23$ cm (width×height×depth). A screw-shaft is used to convert the rotation of the motor to the spring box's linear motion. A system of sprocket gears and chains is then used to transmit that motion into the end-effector, resulting in the angular motion of the back-pad which interacts with a human subject.

During the experiment, a human subject lays down on the bench shown in Fig. 8 and performs a sit-up exercise. The robot is moving accordingly with the subject providing additional support to complete the task. The robot is programmed not to override the human motion, but provide force assistance as needed. The subject is 152 cm tall, and 54 kg. The experiment was repeated ten times for statistical data and the sensory signals were collected.

Each row of the force sensors on the back pad was added together to obtain the total amount of force occurred in each row. During the experimental runs, row 1, 2, and 3 did not generate significant force signals since the human subject's upper back does not touching the force sensors. Sensor rows 4, 5, 6, and 7 recorded significant values which were captured and analyzed in Fig. 9. Due to

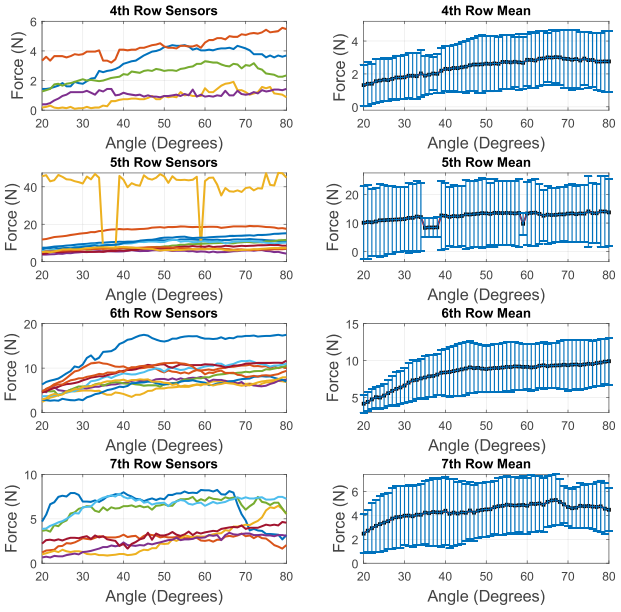

Fig. 9. Force vs Angle for the recorded by the encoder and force sensors.

the nature of the sit-up exercises that lead to the bending of the upper back [39] leaving the spine semi-curved, row 4 and 7 recorded the lowest force while row 5 and 6 recorded the highest in Fig. 9. During the experiments, we observed that the interaction between the human back and the robot's end-effector abound the position of sensor row 5 are not consistent, i.e. sometimes there is no contact. That is the reason why the measurement vary significantly as seen in Fig. 9. As the human subject come closer to their knees, the central nervous system activates more muscles to exert higher force for accomplishing the motion. Therefore, as the angular position increases, the force required to achieve that position also increases. These force measurements demonstrate the amounts of effort contribute by the robot to assist the human subject with the physical exercise.

6. CONCLUSION

We have discussed the design of a bio-assistive robotic system that targets the physical rehabilitation of back-pain, a musculoskeletal problem that imposes a huge burden on societies and health care systems. The main challenge in the development of a robotic rehabilitator is the safe interactions between a human user and the device since human is an integrated part of the cyber-physical loop. To address this challenge, we design the robot with the series-elastic actuation principle that facilitates an elastic coupling, instead of a rigid joint, between an actuator and an end-effector that interacts with a user. This allows the unwanted forces to be absorbed along the compliant elements, and hence, is easier to regulate the impedance of the mechanism. Furthermore, low-stiffness joints and low reflected inertia reduce the risk of the robot hurting the user, while stiffness can also be adjusted to adapt to each patient's recovery profile.

The fundamental hypothesis for the design is that the end-effector produces an elastic force in response to the motion of the input actuator. In addition, the effective stiffness of the elastic coupling can be varied by adjusting the position of the springs. In order to validate the hypothesis, we established a torque model, built a prototype of the design, and perform numerical studies and experiments using the prototype and a robotic manipulator. The results confirm the hypothesis and display agreement between the data produced by the torque model and the data collected from the experiments.

Moreover, we built a full scale model to study the human behavioral interaction with the mechanism. The mechanism aim is to assist the patient in performing the required task while they are exerting 70-80 percentage of their effort to accomplish the motion. It is observed that the proposed mechanism assists the human subject to achieve a desired position, which in return will strength the spinal tendon.

Future work will focus on the control aspects of the robotic rehabilitator. In particular, we will consider the entire robot as a control system with a human user in the loop interacting with a variable-stiffness rehabilitation robot. Such a control system is challenging to handle. To address the challenge, we will look into advanced control techniques, such as the fuzzy controllers for a limb exoskeleton in [40] and the human-robot collaborative controller in [41]. Another direction is to leverage our previous work [42–47] to develop adaptive controllers capable of compensating for neuromotor delay in human-in-the-loop systems, for which the back-pain rehabilitation robot in this paper is a typical example.

REFERENCES

[1] J. Friedly, C. Standaert, and L. Chan, "Epidemiology of spine care: the back pain dilemma," *Physical Medicine and Rehabilitation Clinics*, vol. 21, no. 4, pp. 659-677, 2010.

[2] R. van den Berg, M. de Hooge, F. van Gaalen, M. Reijnierse, T. Huizinga, and D. van der Heijde,"Percentage of patients with spondyloarthritis in patients referred because of chronic back pain and performance of classification criteria: experience from the spondyloarthritis caught early (space) cohort," *Rheumatology*, vol. 52, no. 8, pp. 1492-1499, 2013.

[3] F. Hofmann, U. Stossel, M. Michaelis, M. Nubling, and A. Siegel, "Low back pain and lumbago-sciatica in nurses and a reference group of clerks: results of a comparative prevalence study in germany," *Proc. of In'l Archives of Occupational and Environmental Health*, vol. 75, no. 7, pp. 484-490, 2002.

[4] T. Vos, A. D. Flaxman, M. Naghavi, R. Lozano, C. Michaud, M. Ezzati, *et al.*, "Years lived with disability (ylds) for 1160 sequelae of 289 diseases and injuries 1990-2010: A systematic analysis for the global burden of disease study 2010," *The Lancet*, vol. 380, no. 9859, pp. 2163-2196, 2012.

[5] T. M. Manini, S. L. Hong, and B. C. Clark, "Aging and muscle: a neuron's perspective," *Current Opinion in Clinical Nutrition and Metabolic Care*, vol. 16, no. 1, pp. 21-26, 2013.

[6] W. E. Garrett Jr, "Muscle strain injuries," *The American Journal of Sports Medicine*, vol. 24, no. 6, pp. S2-S8, 1996.

[7] M. Gore, A. Sadosky, B. R. Stacey, K.-S. Tai, and D. Leslie, "The burden of chronic low back pain: clinical comorbidities, treatment patterns, and health care costs in usual care settings," *Spine*, vol. 37, no. 11, pp. 668-677, 2012.

[8] B. I. Martin, R. A. Deyo, S. K. Mirza, J. A. Turner, B. A. Comstock, W. Hollingworth, and S. D. Sullivan, "Expenditures and health status among adults with back and neck problems," *Jama*, vol. 299, no. 6, pp. 656-664, 2008.

[9] P. C. Coyte, C. V. Asche, R. Croxford, and B. Chan, "The economic cost of musculoskeletal disorders in canada," *Arthritis and Rheumatism*, vol. 11, no. 5, pp. 315-325, 1998.

[10] B. Walker, R. Muller, and W. Grant, "Low back pain in australian adults: the economic burden," *Asia Pacific Journal of Public Health*, vol 15, no. 2, pp. 79-87, 2003.

[11] Y. Henchoz, C. Tetreau, J. Abboud, M. Piche, and M. Descarreaux, "Effects of noxious stimulation and pain expectations on neuromuscular control of the spine in patients with chronic low back pain," *The Spine Journal*, vol. 13, no. 10, pp. 1263-1272, 2013.

[12] N. S. Ward and L. G. Cohen, "Mechanisms underlying recovery of motor function after stroke," *Archives of Neurology*, vol. 61, no. 12, pp. 1844-1848, 2004.

[13] S. M. McGill, "Low back exercises: evidence for improving exercise regimens," *Physical Therapy*, vol. 78, no. 7, pp. 754-765, 1998.

[14] C. Liebenson, *Rehabilitation of the Spine a Practitioners Manual*, Lippincott Williams and Wilkins, 2007.

[15] N. Schweighofer, Y. Choi, C. Winstein, and J. Gordon, "Task-oriented rehabilitation robotics," *American Journal of Physical Medicine and Rehabilitation*, vol. 91, no. 11, pp. S270-S279, 2012.

[16] I. Diaz, J. J. Gil, and E. Sanchez, "Lower-limb robotic rehabilitation: literature review and challenges," *Journal of Robotics*, vol. 2011, 2011.

[17] W. Choi, J. Won, H. Cho, and J. Park, "A rehabilitation exercise robot for treating low back pain," *Proc. of IEEE Int'l Conference on Robotics and Automation*, pp. 482-489, 2017.

[18] J. Stein, "Robotics in rehabilitation: technology as destiny," *American Journal of Physical Medicine & Rehabilitation*, vol. 91, no. 11, pp. S199-S203, 2012.

[19] B. Vanderborght, A. Albu-Schaeffer, A. Bicchib, E. Burdet, D. G. Caldwell, R. Carloni, M. Catalano, O. Eiberger, W. Friedl, G. Ganesh, M. Garabini, M. Grebenstein, G. Grioli, S. Haddadin, H. Hoppner, A. Jafari, M. Laffranchi, D. Lefeber, F. Petit, S. Stramigioli, N. Tsagarakis, M. van Damme, R. van Ham, L. C. Visser, and S. Wolf, "Variable impedance actuators: A review," *Robotics and Autonomous Systems*, vol. 61, no. 12, pp. 1601-1614, 2013.

[20] N. Paine, S. Oh, and L. Sentis, "Design and control considerations for high-performance series elastic actuators," *IEEE/ASME Transactions on Mechatronics*, vol. 19, no. 3, pp. 1080-1091, 2013.

[21] C. Lee and S. Oh, "Configuration and performance analysis of a compact planetary geared elastic actuator," *Proc. of IEEE Industrial Electronics Society Conf.*, pp. 6391-6396, 2016.

[22] M. Plooij, M. van Nunspeet, M. Wisse, and H. Vallery, "Design and evaluation of the bi directional clutched parallel elastic actuator (bic-pea)," *Proc. of IEEE Int'l Conference on Robotics and Automation*, pp. 1002-1009, 2015.

[23] K. Kong, J. Bae, and M. Tomizuka, "A compact rotary series elastic actuator for human assistive systems," *IEEE/ASME Transactions on Mechatronics*, vol. 17, no. 2, pp. 288-297, 2011.

[24] B.-S. Kim and J.-B. Song, "Design and control of a variable stiffness actuator based on adjustable moment arm," *IEEE Transactions on Robotics*, vol. 28, no. 5, pp. 1145-1151, 2012.

[25] Y. Xin, Z. C. Qin, and J. Q. Sun, "Robust experimental study of data-driven optimal control for an underactuated rotary flexible joint," *International Journal of Control, Automation and Systems*, vol. 18, no. 1, pp. 1-13, 2019.

[26] S. Fasoli, H. Krebs, and N. Hogan, "Robotic technology and stroke rehabilitation: translating research into practice," *Topics in Stroke Rehabilitation*, vol. 11, no. 4, pp. 11-19, 2004.

[27] P. Lum, D. Reinkensmeyer, and R. Mahoney, "Robotic devices for movement therapy after stroke: current status and challenges to clinical acceptance," *Topics in Stroke Rehabilitation*, vol. 8, no. 4, pp. 40-53, 2002.

[28] C. A. Stanger, C. Anglin, W. S. Harwin, "Devices for assisting manipulation: a summary of user task priorities," *IEEE Transactions on Rehabilitation Engineering*, vol. 2, no. 4, pp. 256-265, 1994.

[29] Z. Shen, Y. Zhuang, J. Zhou, J. Gao, and R. Song, "Design and test of admittance control with inner adaptive robust position control for a lower limb rehabilitation robot," *International Journal of Control, Automation and Systems*, vol. 18, no. 1, pp. 134-142, 2020.

[30] M. Lee, M. Rittenhouse, and H. A. Abdullah "Design issues for therapeutic robot systems: results from a survey of physiotherapists," *Journal of Intelligent and Robotic Systems*, vol. 42, no. 3, pp. 239-252, 2005.

[31] B. Kim, "Analysis on effective rehabilitation of human arms using compliant strap," *Int'l Journal of Control, Automation and Systems*, vol. 16, no. 6, pp. 2958-2965, 2018.

[32] C. Larivière, R. da Silva, A. B. Arsenault, S. Nadeau, A. Plamondon, and R. Vadeboncoeur, "Specificity of a back muscle exercise machine in healthy and low back pain subjects," *Medicine and Science in Sports and Exercise*, vol. 42, no. 3, pp. 592-599, 2010.

[33] W. Choi, J. Won, H. Cho, and J. Park, "A rehabilitation exercise robot for treating low back pain." *Proc. of IEEE Int'l Conference on Robotics and Automation*, pp. 482-489, 2017.

[34] J. M. Hart, J. M. Fritz, D. C. Kerrigan, E. N. Saliba, B. M. Gansneder, and C. D. Ingersoll, "Quadriceps inhibition after repetitive lumbar extension exercise in persons with a history of low back pain," *J. Athletic Training*, vol. 41, no. 3, pp. 264-269, 2006.

[35] N. Kofotolis, E. Kellis, S. P. Vlachopoulos, I. Gouitas, and Y. Theodorakis "Effects of Pilates and trunk strengthening exercises on health-related quality of life in women with chronic low back pain," *Journal of Back and Musculoskeletal Rehabilitation*, vol. 29, no. 4, pp. 649-659, 2016.

[36] R. van Ham, M. van Damme, B. Vanderborght, B. Verrelst, and D. Lefeber, "Maccepa: The mechanically adjustable compliance and controllable equilibrium position actuator," *Proceedings of CLAWAR*, pp. 196-203. 2006.

[37] M. M. R. Hutten and H. J. Hermens "Reliability of lumbar dynamometry measurements in patients with chronic low back pain with test-retest measurements on different days," *European Spine Journal*, vol. 6, no. 1, pp. 54-62, 1997.

[38] B. Hwang and D. Jeon "Estimation of the user's muscular torque for an over-ground gait rehabilitation robot using torque and insole pressure sensors," *Journal of Control, Automation and Systems*, vol. 16, no. 1, pp. 275-283, 2018.

[39] P. Cordo, V. S. Gurfinkel, T. C. Smith, P. W. Hodges, S. M. P. Verschueren, and S. Brumagne, "The sit-up: complex kinematics and muscle activity in voluntary axial movement," *J. Electromyography and Kinesiology*, vol. 13, no. 3, pp. 239-252, 2003.

[40] Z. Li, C. Y. Su, G. Li, and H. Su "Fuzzy approximation-based adaptive backstepping control of an exoskeleton for human upper limbs," *IEEE Transactions on Fuzzy Systems*, vol. 23, no. 3, pp. 555-566, 2014.

[41] H. Su, J. Sandoval, P. Vieyres, G. Poisson, G. Ferrigno, and E. de Momi, "Safety-enhanced collaborative framework for tele-operated minimally invasive surgery using a 7-DoF torque-controlled robot," *International Journal of Control, Automation and Systems*, vol. 16, no. 6, pp. 2915-2923, 2018.

[42] K. D. Nguyen and H. Dankowicz, "Cooperative control of networked robots on a dynamic platform in the presence of communication delays," *Journal of Robust and Nonlinear Control*, vol. 27, no. 9, pp. 1433-1461, 2017.

[43] K. D. Nguyen, Y. Li, and H. Dankowicz, "Delay robustness of an L_1 adaptive controller for a class of systems with unknown matched nonlinearities," *IEEE Trans. on Automatic Control*, vol. 63, no. 10, pp. 5485-5491, 2017.

[44] K. D. Nguyen, "A predictor-based model reference adaptive controller for time-delay systems," *IEEE Trans. on Automatic Control*, vol. 63, no. 12, pp. 4375-4382, 2018.

[45] K. D. Nguyen and H. Dankowicz, "Input-delay compensation in a robust adaptive control framework," *IET Control Theory & Applications*, vol. 13, no. 11, pp. 1718-1727, 2019.

[46] K. D. Nguyen, "Uniform continuity and delay robustness of an adaptive controller for Lagrangian systems," *IMA J. of Mathematical Control and Information*, vol. 37, no. 2, pp. 555-584, 2020.

[47] K. D. Nguyen, "An adaptive compensator for uncertain nonlinear systems with multiple time delays" *Automatica*, vol. 117, 108976, 2020.

ElHussein Shata received his B.S. and M.S. degrees in mechanical engineering from South Dakota State University (SDSU), USA, in 2016 and 2020, respectively. His research interests include variable stiffness actuators, classical control systems, and machine design.

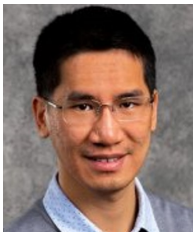

Kim-Doang Nguyen is an Assistant Professor in the Department of Mechanical Engineering at SDSU. He received his Ph.D. degree in mechanical engineering from the University of Illinois at Urbana Champaign (UIUC) in 2015. Between 2015 and 2017, he was a postdoctoral scientist at UIUC and the University of Technology Sydney, Australia. His research interests include control theory, time-delay systems, and robotics.

Praneel Acharya received his B.E. degree from Nanjing University of Aeronautics and Astronautics in 2017. He is currently pursuing a Ph.D. degree in mechanical engineering at SDSU. His research interests include robotic manipulation, motion planning, control, and computer vision.

Jeffrey Doom received his Ph.D. degree from University of Minnesota in 2009. He is currently an Assistant Professor in mechanical engineering at SDSU. His research interests include computational fluid dynamics, fluid mechanics, and modeling and simulation.